New PWM inverter control based on optimal pulse pattern computation without phases symmetry constraints

Adrien Bourgeade, Malek Ghanes, Barbot Jean-Pierre, Bouarfa Abdelkader, Fadel Maurice, Boisliveau Robert

New PWM Inverter Control Based on Optimal Pulse Pattern Computation Without Phases Symmetry Constraints⋆

Adrien Bourgeade[a,*], Malek Ghanes[a], Barbot Jean-Pierre[a,b], Bouarfa Abdelkader[c], Fadel Maurice[d], Boisliveau Robert[a]

[a]*Ecole Centrale de Nantes, LS2N, UMR CNRS 6004, 1 rue de la Noe, BP 92101, Nantes Cedex 3, 44321, France*
[b]*ENSEA, Quartz EA 7393, 6 Av. du Ponceau, Cergy Pontoise, 95000, France*
[c]*Renault Group, Technocentre, 1 Avenue du Golf, Guyancourt, 78280, France*
[d]*ENSEEIHT, LAPLACE, 2, rue Charles Camichel BP 7122, Toulouse Cedex 7, 31071, France*

Abstract

The control of inverters has degrees of freedom that opens the way to improve the output harmonic spectrum. Numerous works dealing with this objective have been proposed in the literature particularly within the definition of switching angles. Among them, the well known PWM techniques such as Quarter Wave Symmetry (QWS), Half Wave Symmetry (HWS) and Full Wave Symmetry (FWS) are based on Optimal Pulse Patterns (OPP) computation using symmetries angles constraints. In this paper in order to improve the harmonic quality, the symmetries angles constraints are not considered leading to a new OPP method: Phases Symmetry Relaxation (PSR). To highlight the interest of the proposed PSR method, an evaluation in terms of Weighted Total Harmonic Distortion (WTHD) is performed. Simulation and experimental tests are conducted in comparison with the well known FWS, highlighting the interest of the proposed PSR strategy.

Keywords: Power electronics, Simulation and Experimental Model Validation, Optimization, Pulse Width Modulation, Optimized pulse patterns, Phase symmetry relaxation.

Nomenclature

Acronyms & Notations

AC/DC	**A**lternative/**D**irect **C**urrent
FWS	**F**ull **W**ave **S**ymmetry
HWS	**H**alf **W**ave **S**ymmetry
IGBT	**I**nsulated-**G**ate **B**ipolar **T**ransistor
ObF	**Ob**jective **F**unction
OPP	**O**ptimal **P**ulse **P**atterns
PSR	**P**hases **S**ymmetry **R**elaxation
PWM	**P**ulse **W**idth **M**odulation
QWS	**Q**uarter **W**ave **S**ymmetry
SHEPWM	**S**elective **H**armonic **E**limination **PWM**
SPWM	**S**inusoidal **P**ulse **W**idth **M**odulation
SVM	**S**pace **V**ector **M**odulation
THD	**T**otal **H**armonic **D**istortion
U.C.	**U**nder **C**onstraints
WTHD	**W**eighted **T**otal **H**armonic **D**istortion

Optimisation parameters and variables

α_i	Angle commutation number i
Δt	Dead-time value
δt_{min}	Minimum time gap between two switching
$\delta\theta_{min}(\omega)$	Minimum electric angle gap $\delta\theta_{min}(\omega) = \omega\delta t_{min}$
ϵ_θ	Angle tolerance
ϵ_V	voltage tolerance
$\mathbf{h}$	Constraint vector
$\mathbf{K}$	Penalty coefficient vector

⋆This work was supported by the project Chair between Renault Group and Centrale Nantes about electric vehicle bidirectional charger control.

*Corresponding author
Email addresses: adrien.bourgeade@ec-nantes.fr (Adrien Bourgeade), malek.ghanes@ec-nantes.fr (Malek Ghanes), barbot@ensea.fr (Barbot Jean-Pierre), abdelkader.bouarfa@renault.com (Bouarfa Abdelkader), maurice.fadel@laplace.univ-tlse.fr (Fadel Maurice), robert.boisliveau@ec-nantes.fr (Boisliveau Robert)

$\mathbf{x}$	Decision variable Matrix ($p \times N_d$)
$\mathbf{x}_Z$	Decision variable vector ($1 \times N_d$), $Z \in [\![1; p]\!]$
$\boldsymbol{\alpha}_{FWS}$	HWS solution vector extended to FWS
$\boldsymbol{\alpha}_{HWS}$	QWS solution vector extended to HWS
$\boldsymbol{\alpha}_{PSR}$	FWS solution vector extended to PSR
$\boldsymbol{\alpha}_{QWS}$	QWS solution vector
θ	Angle variable (electric angle), $\theta = \omega t$
$f(\theta)$	Designate an objective function which depends of θ. In the results sections it designate WTHD
f_s	Switching frequency defined as: $f_s = 2N_{qp}f_1$
f_v	Current objective value with constraints penalties
l_b	Lower bound for the optimisation problem
N_d	Number of decision variables
n_m	Number of harmonics computed
N_{qp}	Number of commutation per quarter period
u_b	Upper bound for the optimisation problem
$x_{Z,k}$	k^{th} element of $\mathbf{x}_Z$, $k \in [1, N_d]$
System parameters	
ω	Fundamental electric pulsation desired $\omega = 2\pi f_1$
E_{DC}	Bus voltage afforded by the battery
f_1	Fundamental electric frequency desired
p	Number of phases of the load
Measures, and analysis	
$\mathbf{a}_{n,I}, \mathbf{b}_{n,I}$	Current Fourier coefficients for harmonic $n \in \mathbb{N}$
$\mathbf{a}_{n,V}, \mathbf{b}_{n,V}$	Voltage Fourier coefficients for harmonic $n \in \mathbb{N}$
$\mathbf{I}_n$	Harmonic current amplitudes vector $n \in [\![2; \infty]\!]$
$\mathbf{V}_1$	Fundamental desired voltage amplitude vector
$\mathbf{V}_n$	Harmonic voltage amplitudes vector $n \in [\![2; \infty]\!]$
$\varphi_{Z,n}$	n^{th} harmonic phase shift for $Z \in [\![1; p]\!]$
$a_{c,n,W}, b_{c,n,W}$	Command Fourier coefficients vector for $W \in \{QWS, HWS, FWS, PSR\}$ and $n \in \mathbb{N}$
$a_{n,Z,V}, b_{n,Z,V}$	Voltage Fourier coefficients for $Z \in [\![1; p]\!]$ and harmonics $n \in \mathbb{N}$
$E_{sw}(i_Z(t))$	Energy lost while switching current $i_Z(t)$
$I_{Z,n}$	n^{th} harmonic current amplitude for $Z \in [\![1; p]\!]$
$i_Z(t)$	Instantaneous current at time t, for $Z \in [\![1; p]\!]$
m	Modulation index
m_{max}	Maximal feasible modulation index $m_{max} = \frac{2}{\pi}$
$P_{con}(i_Z(t))$	Power lost inside the IGBT and the diode because of $i_Z(t)$ current conduction
$V_{Z,n}$	n^{th} harmonic voltage amplitude for $Z \in [\![1; p]\!]$
V_Z	Single voltage of the leg Z, $Z \in [\![1; p]\!]$
Others	
α_{j,m_i}	Angle number j corresponding to m_i
$\boldsymbol{\Psi}_k$	Vector defined as $\boldsymbol{\Psi}_k = [\alpha_{k,m_1}, \cdots, \alpha_{k,m_{imax}}]^t$
$\widehat{\boldsymbol{\Psi}}_k$	Estimated vector of $\boldsymbol{\Psi}_k$
$\mathbf{E}(X)$	Expectation of X
$\mathbf{M_j}$	Vector defined as: $\mathbf{M_j} = [m_0, m_1, \cdots, m_{imax}]^t$
$\widehat{\alpha}_{j,m_i}$	Estimated angle of α_{j,m_i}
m_i	modulation index of the solution number i
m_{imax}	Maximum modulation index number
S_i	Initial command value (high: 1, low: 0)
S_Z	Command for the leg Z, $Z \in [\![1; p]\!]$

Moreover, bold variables represents either matrices or vectors.

1. Introduction

In order to modulate the AC power of an electrical load, an inverter is needed. It will transform a DC signal to an alternative one (voltage to current or current to voltage). This alternative signal is composed of p-phases, with $p \in \mathbb{N}^*$ the phase number of the load. In electrical energy transformation, there are many problems which have to be considered, the first one is a cost problem. This problem often leads to consider a minimum number and cheap semiconductors. For example, this constraint leads to consider only six switches, for the most common inverter, the three phases one. Each switch is composed of an IGBT with a freewheeling diode. For this specific case, this inverter is then composed of three legs, and is commanded by two levels [1].

Carrier based PWM exist since middle of the XX$^{\text{th}}$ century to control power electronic devices such as inverters [2]. Many works tried to improve the PWM by injecting harmonics in the modulated signal [1, 3, 4, 5, 6], or by vector modulation methods [7, 8, 9].

More recently, with the technical progress, the microcontrollers and memory storage improvement. A new PWM class appeared, the off-line ones [10, 11, 12]. This new class is based on the storage of switching angles. The first benefit of this technique is to use all the freedom afforded by the inverter structure. Indeed, previous works[1] show that only two phases are necessary to drive an inverter. Then OPP exploit all the possibilities to find the best PWM strategy possible. One of the other main advantages of OPP, is that their working zone is extended to the modulation index $m_{\max} = \frac{2}{\pi}$, [1]. This extension is significant in comparison with classical symmetries (as SVM or THIPWM$\frac{1}{6}$ for example) limited to $m_{\max} = \frac{1}{\sqrt{3}}$.

The work presented here deals with OPP, these solutions will be used in a control loop to feed an inductive load. Here, the control loop is considered as a black box. Furthermore, the hypothesis that the command provides a correct information is done. Information needed is the desired output signal (current or voltage). Thanks to this information provided, the inverter will work without any feedback and then work in an open-loop mode. Many works treat the global problem of power electronics control in a more global loop without considering the PWM problem [13, 14]. And the purpose of this paper is the opposite one. The Inverter, and furthermore, the PWM are drove and the control loop is ignored. This hypothesis is feasible as the global control loop have not the same purpose than PWM control[1]. The first one is concerned about, speed, torque, observation, etc.. and the second one is concerned about the load harmonics and its impacts [1].

It also exists closed loop PWM[15, 16, 17], but their main disadvantage it they need more sensors or observers (often, voltage ones) to be effective. The OPP, on their side, only need informations already provided by the control loop, as the desired voltage and the motor angle for example.

This paper is concerned about a new open loop OPP with its complete and directly applicable optimization problem. Solutions are proposed for any number of phases p with a two levels inverter. Nevertheless other works treat multilevel converters [18, 19].

The study presented is based on one of the two following main methods used in the literature.

The first one [10, 11, 20, 21, 22, 23, 24, 25] is concerned about minimization of THD or WTHD with different algorithms. Indeed it is very simple to compute harmonic distortion, and, furthermore WTHD is a good way to evaluate current behavior in an inductive load [12]. The weights on harmonics of the WTHD will behave like in an inductive load with the advantage that it do not depends on any physical parameter. This independence to parameters, is the main reason why WTHD is a classical objective function in inverter PWM issues.

Other works are dedicated to SHEPWM. The principle is to select the harmonics to eliminates and then trying to reduce them, [10, 23, 26, 27, 28, 29, 30, 31]. This objective is the second most classic objective function. As SHEPWM seems to be a particular case of WTHD, it is not necessary to study this objective function. Furthermore SHEPWM obliges to choose among all the harmonics which one to eliminate. This choice is quite complex and depend on the considered load and objective.

The following of the paper is concerned about an anteriority study of QWS, HWS and FWS in section 2. The presentation of the PSR is performed in section 3. Thanks to this optimization description a computation method is provided in section 4. Evaluation criteria is presented in section 5. Next, the proposed PSR and the classical FWS are implemented and compared in simulation (section 6) and experimentally (section 7), for the most common inverter $p = 3$.

2. Anteriority background, QWS, HWS and FWS description

In articles [11, 32], it appears that, choosing the angles position inside a same period, with respect to synchronism, affords better results than SVM or carrier based PWM. Indeed choosing precisely switching angles[2] in order to perform the desired voltage or current is known as the best method to solve the optimization tracking problem. Solving this problem is difficult due to the large amount of different solutions. Here after is a Fourier description of the classical angle model depending on different symmetries.

2.1. The angle model

It exists three main types of symmetries (QWS, HWS and FWS)[11].

[1] Even if they have not the same purpose, it is obvious that PWM directly depend on the global control loop as its computation is based on the closed loop reference.

[2] The switching angle is the switching time reported over a period, in order to ignore the signal frequency, for the computation. Here after, "angles" designates a switching angles for the seek of simplicity.

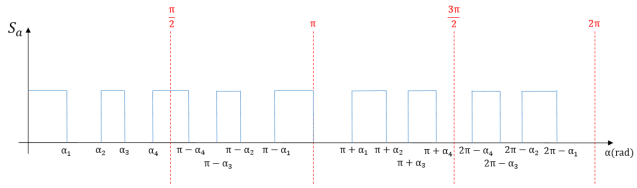

Figure 1: An example of Quarter Wave Symmetry

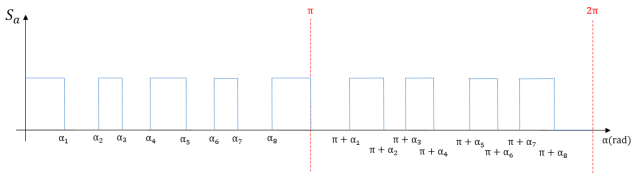

Figure 2: An example of Half Wave Symmetry

As seen on Fig. 1, the principle of the QWS is to select angles of the first quarter period, and then deduce all the others angles of the signal thanks to the known symmetry. The advantage of this solution, resides in the low number of angles to compute. This number is half in comparison with HWS (Fig. 2) and fourth less than FWS (Fig. 3). With the angle knowledge, computation of Fourier coefficients of the formal control (0 or 1), driving the switches is performed, for each symmetry. Then, Fourier decomposition provides a precise expected behavior description of the inverter with only the angle knowledge.

In a real application, and due to the switching of the switches, it is impossible to realize a pure sine wave. However, by imposing the angles on each phase it is possible to minimize the harmonic distortion. [1, 11].

2.1.1. QWS equations

For the QWS strategy the command S_1 is described thanks to the symmetries by $a_{c,0,QWS} = \frac{1}{2}$ and $a_{c,n,QWS} = 0\ \forall n \in [\![1;\infty]\!]$ and $b_{c,n,QWS}$ is defined by eq. (1). Harmonics multiples of two are systematically removed due to the $\left(1+(-1)^{n+1}\right)$ term.

$$b_{c,n,QWS} = \frac{1}{n\pi}(-1)^{S_i}\left(1+(-1)^{n+1}\right)\left(2\sum_{j=1}^{N_{qp}}(-1)^{j+1}\cos(n\alpha_j)-1\right) \quad (1)$$

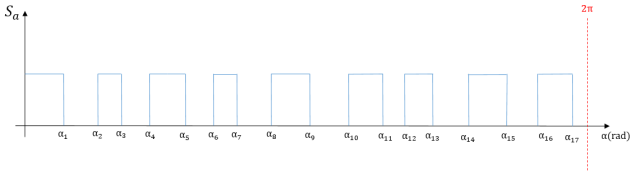

Figure 3: An example of Full Wave Symmetry

2.1.2. HWS equations

For the HWS strategy, $a_{c,0,HWS} = 1$, $a_{c,n,HWS}$ is defined by eq. (2) and $b_{c,n,HWS}$ by eq. (3). As for the QWS the $\left(1+(-1)^{n+1}\right)$ term will remove all the harmonics multiples of two.

$$a_{c,n,HWS} = \frac{1}{n\pi}(-1)^{S_i+1}\left(1+(-1)^{n+1}\right)\left(\sum_{j=1}^{2N_{qp}}(-1)^{j+1}\sin(n\alpha_j)\right) \quad (2)$$

$$b_{c,n,HWS} = \frac{1}{n\pi}(-1)^{S_i}\left(1+(-1)^{n+1}\right)\left(\sum_{j=1}^{2N_{qp}}(-1)^{j+1}\cos(n\alpha_j)-1\right) \quad (3)$$

2.1.3. FWS equations

For the FWS strategy, $a_{c,0,FWS}$, $a_{c,n,FWS}$ and $b_{c,n,FWS}$ are respectively defined by eqs. (4)-(6). Here the harmonics multiples of two, are not systematically removed due to the full period symmetry.

$$a_{c,0,FWS} = \frac{1}{\pi}(-1)^{S_i+1}\left(\sum_{j=1}^{4N_{qp}+1}(-1)^{j+1}\alpha_j + 2\pi\right) \quad (4)$$

$$a_{c,n,FWS} = \frac{1}{n\pi}(-1)^{S_i+1}\left(\sum_{j=1}^{4N_{qp}+1}(-1)^{j+1}\sin(n\alpha_j)\right) \quad (5)$$

$$b_{c,n,FWS} = \frac{1}{n\pi}(-1)^{S_i}\left(\sum_{j=1}^{4N_{qp}+1}(-1)^{j+1}\cos(n\alpha_j)-1\right) \quad (6)$$

Then, with the previous equations, after the inverter computation some harmonics will be removed (equal to zero). Indeed, for a p-phases inverter, harmonics multiple of p will be removed, for the seek of completeness it is demonstrate here after, even if the demonstration is well known in the literature [1].

Let's assume the leg command number k is described by:

$$\begin{aligned} C_{0,k}(\theta) &= a_{0,k} + \sum_{n\geq 1} a_{n,k}\cos\left(n\left(\theta+k\phi\right)\right) \\ &+ b_{n,k}\sin\left(n\left(\theta+k\phi\right)\right) \end{aligned} \quad (7)$$

The voltage of the first leg of a p-phases load can then be described by eq. (10) thanks to matrix defined by eq. (8) multiplied by vector of components eq. (7). Remark, as the $a_{0,k}$ are equals, the resulting mean voltage is equal to 0, $\frac{p-1}{p}a_{0,1} - \frac{1}{p}\sum_{i=1}^{p-1} a_{0,i} = 0$.

$$M = \frac{1}{p}\begin{pmatrix} p-1 & -1 & \cdots & -1 \\ -1 & p-1 & \cdots & -1 \\ \vdots & & \ddots & \vdots \\ -1 & \cdots & -1 & p-1 \end{pmatrix} \quad (8)$$

Voltage of all the phases can be deduced from the command thanks to (7) and (8) and is written as follow.

$$\begin{pmatrix} V_1(\theta) \\ V_2(\theta) \\ \vdots \\ V_p(\theta) \end{pmatrix} = E_{DC} \cdot M \cdot \begin{pmatrix} C_{0,1}(\theta) \\ C_{0,2}(\theta) \\ \vdots \\ C_{0,p}(\theta)(\theta) \end{pmatrix} \tag{9}$$

With the previous equation (9), voltage of the first phase is written as (10).

$$\begin{aligned} V_1(\theta) \quad &= \quad E_{DC}\frac{p-1}{p}\sum_{n\geq 1} a_{n,1}\cos(n\theta) + b_{n,1}\sin(n\theta) \\ &-\tfrac{E_{DC}}{p} \quad \sum_{n\geq 1} a_{n,2}\cos(n\theta + n\phi) + b_{n,2}\sin(n\theta + n\phi) \\ &\quad \cdots \\ &-\tfrac{E_{DC}}{p} \quad \sum_{n\geq 1} a_{n,p}\cos(n\theta + n(p-1)\phi) \\ &+ \quad b_{n,p}\sin(n\theta + n(p-1)\phi) \end{aligned} \tag{10}$$

With $\phi = -\frac{2\pi}{p}$.

$$\begin{aligned} V_1(\theta) \quad &= \quad E_{DC}\frac{p-1}{p}\sum_{n\geq 1} a_{n,1}\cos(n\theta) \\ &+ \quad b_{n,1}\sin(n\theta) \\ &-\tfrac{E_{DC}}{p} \quad \sum_{n\geq 1} a_{n,2}\cos(n\theta)\cos(n\phi) \\ &- \quad a_{n,2}\sin(n\theta)\sin(n\phi) \\ &- \quad b_{n,2}\sin(n\theta)\cos(n\phi) \\ &- \quad b_{n,2}\cos(n\theta)\sin(n\phi) \\ &\quad \cdots \\ &-\tfrac{E_{DC}}{p} \quad \sum_{n\geq 1} a_{n,p}\cos(n\theta)\cos(n(p-1)\phi) \\ &- \quad a_{n,p}\sin(n\theta)\sin(n(p-1)\phi) \\ &+ \quad b_{n,p}\sin(n\theta)\cos(n(p-1)\phi) \\ &+ \quad b_{n,p}\cos(n\theta)\sin(n(p-1)\phi) \end{aligned} \tag{11}$$

For $n = p$, $\cos(n\phi) = 1$ and $\sin(n\phi) = 0$, then the harmonics of rank $n = p$ of the voltage are systematically removed. This demonstration can be done for each phase from 1 to p.

2.2. Problem modeling

In order to find the best angles solutions, for all the classical symmetries, an optimization problem description is needed. Its purpose is to minimize an objective function f chosen.
Remark: WTHD is the objective function in the discussion of this paper.

$$\begin{cases} ObF & \min(f(\mathbf{x})) \\ U.C. & \alpha_k \leq \alpha_{k+1} + \delta\theta_{min}(\omega) \quad \forall k \in [\![1; N_d]\!] \\ & \alpha_{N_d} \leq u_b \\ & \alpha_1 \geq l_b \\ & a_{1,V} = 0 \\ & b_{1,V} = m \end{cases} \tag{12}$$

symmetries	N_d	l_b	u_b
QWS	N_{qp}	$\delta\theta_{min}(\omega)$	$\frac{\pi}{2} - \frac{\delta\theta_{min}(\omega)}{2}$
HWS	$2N_{qp}$	$\delta\theta_{min}(\omega)$	$\pi - \delta\theta_{min}(\omega)$
FWS	$4N_{qp} + 1$	$\delta\theta_{min}(\omega)$	$2\pi - \delta\theta_{min}(\omega)$

Table 1: Optimization problem parameters

In the optimization problem eq. (12), there are two nonlinear constraints, because they depend of the Fourier decomposition, where a lot of trigonometric functions appears. Here, m designates the modulation index, defined as the percentage of use of the DC bus. In the case of a voltage source modulation index is equal to $m = \frac{V_1}{E_{DC}}$, with V_1 the desired voltage amplitude and E_{DC} the bus voltage.

In table 1 let's remark that l_b and u_b are not equal to the theoretical bounds. The reason is technological, as the switches gap, $\delta\theta_{min}$, must be taking into account in the bounds. Another remark, is with problem defined in (12), it is only necessary to focus on the first phase, because all the $p-1$ other phases will be deduced from this one. It is also the reason why the fundamental real part of the Fourier decomposition ($a_{1,V}$) is equal to zero. This leads to the main assumption of classical strategies (QWS, HWS and FWS), that is, angles of each phase are phase shifted symmetrically according to the first phase angles.

As demonstrated before, this angle phase shift affords the advantage to eliminate harmonics multiple of p. On the other hand, this limits the number of solutions. Consequently solutions could be sub-optimal with respect to the set of possible solutions. Next section will focus on this problem consideration.

3. Phases Symmetry Relaxation method

The purpose of PSR method is to relax the angle phase shift constraint. As Birth [11] showed that an angle symmetry relaxation in a single phase improves the harmonic quality. The decision has been done to also do not consider the angle symmetry between phases. As an illustration of the proposed hypothesis relaxation, Fig. 4 highlights a particular case of the angle phase shift relaxation for three phases only. Doing so, the solution set is expanded. Nevertheless the symmetry between voltage (or current) phases will be imposed by constraints on the optimization problem, with respect to a specific precision.

Without the symmetric assumption, the optimization problem is now written like eq. (15). The idea, here, is to find an optimal solution for the angles, according to a chosen objective function f (in this paper, the WTHD). This relaxation of the constraints increases the WTHD quality of the solutions as it will be shown in the sections 6 and 7.

3.1. Problem modeling

From the relaxations way of thinking, a new optimization setting is proposed, generating new freedom degrees and also extra constraints. Then three types of conditions must be met. First, the angle between two switches cannot be lower than a minimal angle $\delta\theta_{min}(\omega)$. This constraint will prevent narrow

pulses and allows switches to commute properly with respect to the dead-time ($\delta\theta_{min}(\omega) > 2\omega\Delta t$). Remark that, a narrow pulse is a pulse lower than the minimal angle ($\delta t_{min} > 2\Delta t$).

Secondly, angles are bounded on a period, theoretically it would be 0 to 2π and practically see table 2. Those two conditions together correspond to $4\left(N_{qp}+1\right)$ linear constraints.

Finally, all the optimized output signals must respect the correct amplitude and phase for the fundamental. Explaining why the $3p$ nonlinear equalities constraints eq. (13) and eq. (14) must be verified.

$$\sqrt{a_{1,V}^2 + b_{1,V}^2} = m \pm \epsilon_V \tag{13}$$

$$\tan(-\frac{2(Z-1)\pi}{p} \pm \epsilon_\theta) = \frac{b_{1,Z,V}}{a_{1,Z,V}}, \quad \forall Z \in \{1,2,\cdots,p\} \tag{14}$$

Remark: For the particular case presented in section 6 and 7, the equality constraint equations of the optimization problem are imposed to be precise at 2% on the amplitude and of $\frac{\pi}{25}$ on phases.

The optimization problem, is now the following one with the same objective function as 12:

$$\begin{cases} ObF & \min(f(\mathbf{x})) \\ U.C. & \mathbf{x} = [\mathbf{x_1}, \mathbf{x_2}, \cdots, \mathbf{x_p}] \\ & x_{1,k} \leq x_{1,k+1} + \delta\theta_{min}(\omega) \\ & x_{2,k} \leq x_{2,k+1} + \delta\theta_{min}(\omega) \\ & \cdots \\ & x_{p,k} \leq x_{p,k+1} + \delta\theta_{min}(\omega) \\ & x_{1,4N_{qp}+2} \leq u_b, \\ & x_{2,4N_{qp}+2} \leq u_b, \cdots \\ & x_{p,4N_{qp}+2} \leq u_b \\ & x_{1,1} \geq l_b, \;\; x_{2,1} \geq l_b, \cdots, \;\; x_{p,1} \geq l_b \\ & a_{0,1,V} = 0, \;\; a_{0,2,V} = 0, \cdots, \;\; a_{0,p,V} = 0 \\ & a_{1,1,V} = 0 \\ & a_{1,2,V} = m\sin(-\frac{2\pi}{p}), \cdots \\ & a_{1,p,V} = m\sin(-2\pi\frac{p-1}{p}) \\ & b_{1,1,V} = m, \\ & b_{1,2,V} = m\cos(-\frac{2\pi}{p}), \cdots \\ & b_{1,p,V} = m\cos(-2\pi\frac{p-1}{p}) \end{cases} \tag{15}$$

To analyze the command performances of the PSR, same equations than for the FWS are used. Precisely, eq. (4), eq. (5) and eq. (6) are the same for PSR, except that j vary between 1 and $4N_{qp}+2$. Here the symmetry between the angles is not forced by a deduction from a single phase. Then no harmonics will be forced to be equal to zero, which is the main difference with FWS. Remark that in the problem eq. (15), $k \in [\![1, 4N_{qp}+2]\!]$. It appears there is one more switching in comparison with FWS and two more switching in comparison with QWS and HWS. The first additional switching is due to the symmetry which requires to have a switching in π (see Fig. 1 and Fig. 2). The second additional switching is due to the 2π symmetry, this commutation is present in every classical symmetry (see Fig. 1, Fig. 2 and Fig. 3). This 2π periodicity is the reason why an extra switching appears at the end of the period.

	N_d	l_b	u_b
PSR	$3(4N_{qp}+2)$	$\delta\theta_{min}$	$2\pi - \delta\theta_{min}$

Table 2: PSR Optimization problem parameters

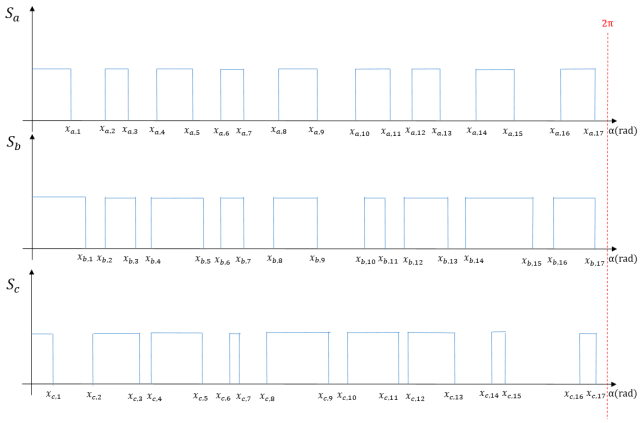

Figure 4: Three phases inverter example of PSR strategy

Concerning the dead-time (Δt), it is naturally implemented during the experiences to avoid short circuits. Nevertheless it is neglected on (15) to simplify the WTHD computation. Indeed precise knowledge on dead-time influence is quite complex as presented in [33]. This claim is confirmed under the hypothesis of $f_1\Delta t << 1$, which verifies the first order development of the S_Z Fourier decomposition and gives (16) and (17).

$$\widetilde{a}_{c,n,FWS} = a_{c,n,FWS} - \frac{\omega\Delta t}{\pi}(-1)^{S_i}\left(\sum_{j=1}^{4N_{qp}+1}\cos(n\alpha_j)\right) + o(\Delta t^2) \tag{16}$$

$$\widetilde{b}_{c,n,FWS} = b_{c,n,FWS} - \frac{\omega\Delta t}{\pi}(-1)^{S_i}\left(\sum_{j=1}^{4N_{qp}+1}\sin(n\alpha_j)\right) + o(\Delta t^2) \tag{17}$$

Where $\widetilde{a}_{c,n,FWS}$ and $\widetilde{b}_{c,n,FWS}$ are the Fourier coefficient with dead-time effect. So under the assumption $f_1\Delta t << 1$, equations (16) and (17) gives $\widetilde{a}_{c,n,FWS} \approx a_{c,n,FWS}$ and $\widetilde{b}_{c,n,FWS} \approx b_{c,n,FWS}$. Consequently as to take in consideration the dead time on the FWS's WTHD equation and on PSR, this increases the complexity of the computation. It is why Δt is neglected in this paper. Nevertheless, if dead-time consideration is necessary to take in account in future works, it would be done by modifying (15) and δt_{min}.

4. Computation Method

In order to compute an optimization solution, fmincon from the optimization toolbox of MatLab (MathWorks®) is used. Because the workspace has many local minimums, it is necessary to correctly select starting points of fmincon.

The first step, before optimization, starts by creating some random initial points. After that an evaluation of the quality of each point is performed with eq. (18). This equation considers the current value of the objective function, f, which is modified to f_v, in order to respects the constraints.

The initial decision matrix $\boldsymbol{x}_0$ is considered as an appropriate starting point, with respect to f_v, if the solutions has a good fitness (a low $f(\boldsymbol{x}_0)$) and which violate a minimum of nonlinear constraints (K_2 term) and not deeply (K_1 term). Linear constraints are not considered in eq. (18) because they are forced to be verified in the initial matrix. Indeed it is easy to generate a random sorted and bounded matrix.

$$f_v = f(\boldsymbol{x}_0) + K_1 \sum_{i=1}^{3p} (\max(c_i, 0)) + K_2 \sum_{i=1}^{3p} g(c_i) \tag{18}$$

Where $\boldsymbol{x}_0 = [\mathbf{x_{10}}, \mathbf{x_{20}}, \cdots, \mathbf{x_{p0}}]$ is the initial decision matrix, K_1 and K_2 are two penalty coefficients (In sections 6 and 7, K_1 and K_2 are chosen equal to 10^6). Furthermore, g is defined as follow:

$$g(c_i) = \begin{cases} 1 & \text{if } c_i > \epsilon \\ 0 & \text{otherwise} \end{cases} \tag{19}$$

Moreover $\boldsymbol{c} = \left(c_1, c_2 \cdots, c_{3p}\right)$ is the vector of nonlinear constraints, these constraints are the same than for the problem eq. (15). Equation (18) is inspired by the work of Sierra et al. [34].

The first penalty (K_1 term) of eq. (18) indicates how far away the solutions are from the acceptable domain[3] and the second penalty (K_2 term) indicates how many constraints are outside the acceptable domain.

After computing eq. (18), to a large quantity of initial matrices, a selection of the initial matrix with the minimal f_v is done. Then this matrix is considered as a starting matrix for the optimization problem defined by eq. (15), computed for example with fmincon. Furthermore, in order to refine the solution quality, other starting matrices are considered. Three of these starting matrices are found by doing an extension of the previous symmetries. So QWS is extended to HWS eq. (20), the HWS to compute FWS eq. (21) and FWS to PSR eq. (22). This leads to the following extension of symmetries.

$$\boldsymbol{\alpha}_{HWS} = [\alpha_{QWS,1}, \cdots, \alpha_{QWS,N}, \pi - \alpha_{QWS,N}, \cdots, \pi - \alpha_{QWS,1}] \tag{20}$$

$$\boldsymbol{\alpha}_{FWS} = [\alpha_{HWS,1}, \cdots, \alpha_{HWS,2N}, \pi, \pi + \alpha_{HWS,1}, \cdots, \pi + \alpha_{HWS,2N}] \tag{21}$$

[3]The acceptable domain is the domain where the constraints are respected according to prefixed tolerance

$$\boldsymbol{\alpha}_{PSR} = [\boldsymbol{\alpha}_{FWS};\ \text{sort}((\boldsymbol{\alpha}_{FWS} - \frac{2\pi}{3}) \bmod 2\pi); \text{sort}((\boldsymbol{\alpha}_{FWS} - \frac{4\pi}{3}) \bmod 2\pi)\ ] \tag{22}$$

A scheme of the proposed algorithm is given in Fig. 5. This algorithm computes the optimal switching angles of the PSR method from the N_m desired signals depending on the modulation index. If the index of the initial step j is lower than N_m the algorithm stops. Otherwise, as explained previously, an initial matrix $\mathbf{x_0}$ is selected (eq. (18)) and stored in $L_{x_0,j}$, from a random set of matrices $\mathbf{x}$. Then for each element i among the $n_{L,j}$ matrices of $L_{x_0,j}$, an optimization is performed from $L_{x_0,j,i}$. Next, the best solution found among all the starting matrices is selected and stored in Σ_{fin} (the set of final solutions for each modulation indexes). The solution is also stored in $L_{x_0,j+1}$, the next step set of starting matrices and $i = i + 1$. This part of the algorithm stops when i is greater than $n_{L,j}$ and then $j = j + 1$, and the algorithm go to the $j \leq N_m$ test. In order to preserve at least local minimum found from the previous step of the algorithm. The solution from the previous modulation index is also chosen as a starting matrix. It can be seen on Fig. 5 where the j$^{\text{th}}$ solution is stored in the starting matrix list for the next modulation index $L_{x_{0,j+1}}$.

Remark: All the results are obtained with a discretization step of 0.001 and then, the solution found for $m = 0.5$, will be one of the starting matrix of the computation for the next discretization step $m = 0.501$.

5. Evaluation criteria

To evaluate the predicted losses inside the converter and the load. A current, respectively voltage computation is needed, indeed current respectively voltage value is responsible of switches losses, losses inside the load, torque, etc..

5.1. WTHD

5.1.1. Inductive load

A lot of studies are based on WTHD, because it does not depends on a load and allows to evaluate the solution quality quite fast and easily. WTHD is an approximation of all the currents norm inside the inductive load. This load is composed with an inductance L with a resisting part R, subject to a voltage signal of pulsation ω. Note that, through out the paper $L\omega$ and R are constant.

WTHD is the norm of all the harmonics currents in a case of purely inductive load ($R = 0$). In the case of only inductive load, WTHD is an approximation of the current norm. The approximation depends on the value of $\frac{R}{L\omega} << 1$. This condition is justified by the demonstration below [12].

Current can be expressed as the first order differential equation eq. (23). $\mathbf{I}(t) = \left[i_1(t), i_2(t), \cdots, i_p(t)\right]^t$ is the vector of the current in the load p phases. $\mathbf{V}(t) = \left[v_1(t), v_2(t), \cdots, v_p(t)\right]^t$ is the simple voltage vector (output of the inverter to neutral point voltage) in the p phases.

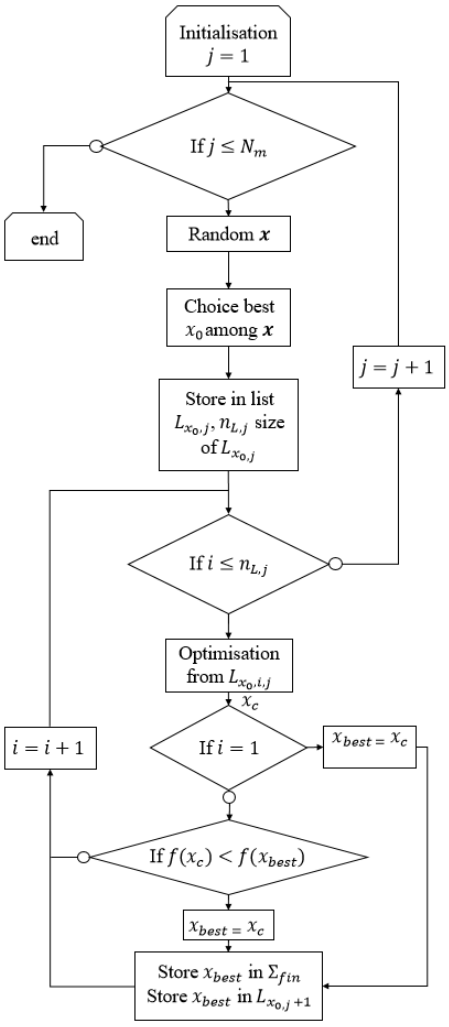

Figure 5: Schematic view of the computation algorithm, N_m is the number of modulation index considered and Σ_{fin} is the final set of solutions found by the algorithm

It is important to notify that in the next demonstration, square roots, multiplication and divisions of vectors are assumed to be term to term. The following demonstration is similar to the Hartgenbusch one [12]. Nevertheless, in order to be self contend a short similar demonstration is presented here after.

$$\frac{d\mathbf{I}(t)}{dt} = \frac{\mathbf{V}(t)}{L} - \frac{R}{L}\mathbf{I}(t) \tag{23}$$

Thanks to the periodic property of the voltage and current, and without considering the dead-time influence for the voltage computation, it is possible to decompose the signal with Fourier series.

$$\mathbf{V}(t) = \mathbf{a}_{0,V} + \sum_{n\geq 1} \mathbf{a}_{n,V}\cos(n\omega t) + \mathbf{b}_{n,V}\sin(n\omega t) \tag{24}$$

$$\mathbf{I}(t) = \mathbf{a}_{0,I} + \sum_{n\geq 1} \mathbf{a}_{n,I}\cos(n\omega t) + \mathbf{b}_{n,I}\sin(n\omega t) \tag{25}$$

$$\frac{d\mathbf{I}(t)}{dt} = \sum_{n\geq 1} n\omega\mathbf{b}_{n,I}\cos(n\omega t) - n\omega\mathbf{a}_{n,I}\sin(n\omega t) \tag{26}$$

On the equation below, Fourier coefficient are p components vectors, each for one phase.

Equations (23) to (26) lead to eq. (27)

$$\begin{cases} \mathbf{0} &= \frac{1}{L}\mathbf{a}_{0,V} - \frac{R}{L}\mathbf{a}_{0,I} \\ n\omega\mathbf{b}_{n,I} &= \frac{1}{L}\mathbf{a}_{n,V} - \frac{R}{L}\mathbf{a}_{n,I} \\ n\omega\mathbf{a}_{n,I} &= \frac{R}{L}\mathbf{b}_{n,I} - \frac{1}{L}\mathbf{b}_{n,V} \end{cases} \tag{27}$$

and then:

$$\begin{cases} \mathbf{a}_{0,I} &= \frac{1}{R}\mathbf{a}_{0,V} \\ \mathbf{a}_{n,I} &= \frac{1}{R^2+(nL\omega)^2}\left(R\mathbf{a}_{n,V} - nL\omega\mathbf{b}_{n,V}\right) \\ \mathbf{b}_{n,I} &= \frac{1}{R^2+(nL\omega)^2}\left(nL\omega\mathbf{a}_{n,V} + R\mathbf{b}_{n,V}\right) \end{cases} \tag{28}$$

Finally, considering $nL\omega >> R \quad \forall n \in \mathbb{N}^*$, current Fourier decomposition can be approximated with eq. (29).

$$\begin{cases} \mathbf{a}_{0,I} &= \frac{1}{R}\mathbf{a}_{0,V} \\ \mathbf{a}_{n,I} &\simeq -\frac{\mathbf{b}_{n,V}}{nL\omega} \\ \mathbf{b}_{n,I} &\simeq \frac{\mathbf{a}_{n,V}}{nL\omega} \end{cases} \tag{29}$$

With this approximation amplitude of each current harmonic ($\mathbf{I}_n$) is given by eq. (30). As $L\omega$ is a constant, let's define $\mathbf{I}'_n = L\omega\mathbf{I}_n$. Indeed a constant do not influence direction of variation of the current.

Remembering that the harmonics must be eliminated or at least reduced, computation will be then performed thanks to $\mathbf{I}'_n$ instead of $\mathbf{I}_n$, both equations are described below.

$$\mathbf{I}_n = \sqrt{\mathbf{a}_{n,I}^2 + \mathbf{b}_{n,I}^2} \quad \forall n \in \mathbb{N}^* \tag{30}$$

$$\mathbf{I}'_n = \frac{1}{n}\sqrt{\mathbf{a}_{n,V}^2 + \mathbf{b}_{n,V}^2} \quad \forall n \in \mathbb{N}^* \tag{31}$$

Remark that in eq. (31) the Fourier coefficients are with respect to voltage instead of current as eq. (30).

Moreover $\mathbf{I}'_n$, can be described with respect to voltage amplitude:

$$\mathbf{I}'_n = \sqrt{\frac{\mathbf{V}_n^2}{n^2}} \quad \forall n \in [\![2; \infty[\![\tag{32}$$

Finally, in order to have a scalar criteria, norm of all the $\mathbf{I}'_n$ for each phase is performed with eq. (33).

$$\|\mathbf{I}'_n\| = \sqrt{\sum_{n>1} \mathbf{I}_n'^2} = \sqrt{\sum_{n>1} \frac{\mathbf{V}_n^2}{n^2}} \tag{33}$$

From eq. (33) the WTHD equation is written for each phase as following:

$$\mathbf{V}_{\text{WTHD},\%} = \frac{100}{\mathbf{V}_1}\|\mathbf{I}'_n\| = \frac{100}{\mathbf{V}_1}\sqrt{\sum_{n>1} \frac{\mathbf{V}_n^2}{n^2}} \tag{34}$$

Under the assumption that angles from each phase are independent eq. (34) and to reduce to a scalar, mean value of the WTHD is computed below.

$$V_{\text{WTHD},\%} = \frac{1}{p}\frac{100}{V_1}\sum_{i=1}^{p}\sqrt{\sum_{n>1} \frac{\mathbf{V}_{n,i}^2}{n^2}} \tag{35}$$

In previous equation, $\mathbf{V}_1$ becomes V_1, because all the terms of the vector are equals and the vector division is done term to term. Finally, eq. (35) provides the WTHD considered as an objective function f in the optimization problem described with eq. (15).

5.1.2. Capacitive load

According to a capacitive load, and then a current source, eq. (23) will be transformed to equation (36).

$$\frac{d\mathbf{V}(t)}{dt} = \frac{\mathbf{I}(t)}{C} - \frac{1}{RC}\mathbf{V}(t) \tag{36}$$

With the same way of thinking, WTHD of eq. (34) becomes eq. (37)

$$\mathbf{I}_{\text{WTHD},\%} = \frac{100}{\mathbf{I}_1}\sqrt{\sum_{n\geq 2} \frac{\mathbf{I}_n^2}{n^2}} \tag{37}$$

As for its voltage counterpart, the considered current WTHD is finally written as:

$$I_{\text{WTHD},\%} = \frac{1}{p}\frac{100}{I_1}\sum_{i=1}^{p}\sqrt{\sum_{n\geq 2} \frac{\mathbf{I}_{n,i}^2}{n^2}} \tag{38}$$

Consequently for capacitive load, eq. (38) provides the WTHD, considered as an objective function f in the optimization problem described with eq. (15).

Because the angles are set precisely with an OPP strategy, it exist a risk that between two angle sets with a near operating point, the angles are strongly different. This problem must have to be considered, indeed, a non homogeneous set of angles will generate strong discontinuities in the inverter. It is why, in the next section a way to evaluate smoothness quality is investigated.

5.2. Smoothness

This section is concerned to present a load independent criteria in order to decide if the smoothness of the angle set can be considered as good or poor. In other terms: What influence will have a tiny mistake on angles on the voltage or current load behavior? To evaluate this influence, a polynomial regression is done on the switching angles, the idea behind is, if the variation for a specific angle is polynomial than its smoothness is considered as a good one.

In the following a precise methodology to evaluate this smoothness is presented. This methodology provides a number based on all the solutions found for a single symmetry. For OPP, decision variable in the algorithm is a vector or a matrix for PSR. Considering all the operating points a matrix could be establish where each line is a set of angle for a specific modulation index. Then a search for a polynomial equation eq. (39) of a specific order n is performed which fit a maximum with the evolution of an angle. Finally the correlation factor between estimated angles with a polynomial function and the real angles set is computed eq. (42). This number will be called the smoothness factor.

If the smoothness factor is close to 1 (a good smoothness) that mean that the two curves (the one described by eq. (39) and the solution set) are similar. The angle evolution can be then approximated by a polynomial equation of the specific order n. Otherwise correlation factor near 0, means there is no correlation between the computed curve and the real one. Then a degradation of the selected objective function must be considered in order to increase smoothness factor.

$$\mathcal{P}(m) = c_n m^n + c_{n-1}m^{n-1} + \cdots + c_0 \tag{39}$$

Where $c_i \ \forall i \in [\![0; n]\!]$ are computed with eq. (40). Note that in this equation the multiplication is a usual one of matrix by a vector. Consequently the Hankel matrix composed of H_j have to be inverted thanks to the pseudo-inverse matrix of Moore-Penrose because the H_j matrix is not regular. Then the chosen estimated angles minimize the euclidean norm to the angles computed with the algorithm (15).

$$\begin{bmatrix} H_0 & \cdots & H_n \\ H_1 & \cdots & H_{n+1} \\ \vdots & \ddots & \vdots \\ H_n & \cdots & H_{2n} \end{bmatrix} \cdot \begin{bmatrix} c_0 \\ c_1 \\ \vdots \\ c_n \end{bmatrix} = \begin{bmatrix} T_0 \\ T_1 \\ \vdots \\ T_n \end{bmatrix} \tag{40}$$

Where T_j and H_j are defined in eq. (41)

$$\begin{cases} T_j = \sum_{i=1}^{n} m_i^j \alpha_{j,m_i} \\ H_j = \sum_{i=1}^{n} m_i^j \end{cases} \tag{41}$$

As $\mathbf{\Psi}_k = [\alpha_{k,m_1}, \cdots, \alpha_{k,m_{imax}}]^t$ a vector of m_{imax} dimensions of the angle number k computed with the problem defined with eq. (15). On the other hand $\widehat{\mathbf{\Psi}}_k$ is a vector of estimated values of $\mathbf{\Psi}_k$, according to the solution found by eq. (39), $\widehat{\mathbf{\Psi}}_k = \left[\mathcal{P}(m_1), \ \mathcal{P}(m_2), \ \cdots, \ \mathcal{P}(m_{max})\right]^t = \left[\hat{\alpha}_{k,m_1}, \ \hat{\alpha}_{k,m_2}, \ \cdots, \ \hat{\alpha}_{k,m_{max}}\right]^t$.

Parameter	value
ϵ_θ	$\pm\pi/25$rad
ϵ_V	$\pm 2mE_{DC}/100$V
K_1, K_2	10^6
δt_{min}	$1\mu s$
n_m	300
E_{DC}	400V
f_1	50Hz

Table 3: Values of the parameters in order to find the presented results

$$r_k = 100\frac{\left(\mathbf{E}(\mathbf{\Psi_k}\widehat{\mathbf{\Psi}}_\mathbf{k}) - \mathbf{E}(\mathbf{\Psi_k})\mathbf{E}(\widehat{\mathbf{\Psi}}_\mathbf{k})\right)^2}{\left(\mathbf{E}(\mathbf{\Psi}_\mathbf{k}^2) - \mathbf{E}(\mathbf{\Psi_k})^2)(\mathbf{E}(\widehat{\mathbf{\Psi}}_\mathbf{k}^2) - \mathbf{E}(\widehat{\mathbf{\Psi}}_\mathbf{k})^2\right)} \quad (42)$$

Where r_k is the smoothness factor.

In order to highlight the well founded of the proposed method (i.e. optimization problems and criteria) an example of computation is proposed in the next section on a three phase voltage inverter.

6. Simulation results

6.1. WTHD comparison

The WTHD comparison, in simulation, is done with respect to the parameters given by table 3. In this section, only FWS and PSR are presented because Birth's paper [11] showed the superiority of FWS over the QWS and HWS. Note that this superiority has been also found while the investigations but are not presented here.

Because the more N_{qp} is great, the more a QWS consideration is enough to obtain good results, the decision have been done to limit the computation to $N_{qp} = 5$. Furthermore, the choice have been done to consider only a three phases voltage inverter in order to highlight the well founded of the proposed method.

In the Fig. 6 and Fig. 7 WTHD comparison are shown respectively for $N_{qp} = 2$ and $N_{qp} = 5$.

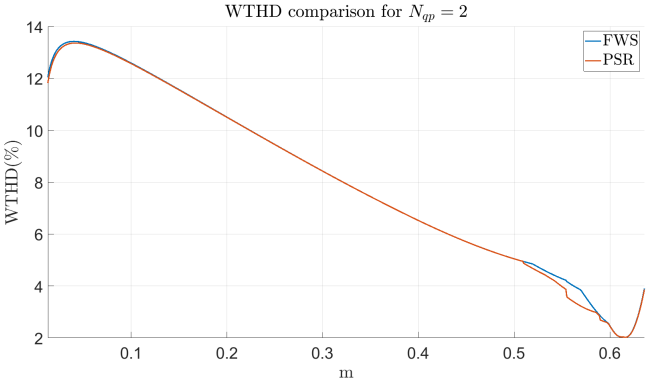

Figure 6: Comparison between FWS and PSR method according to WTHD for $N_{qp} = 2$ when the objective function is WTHD

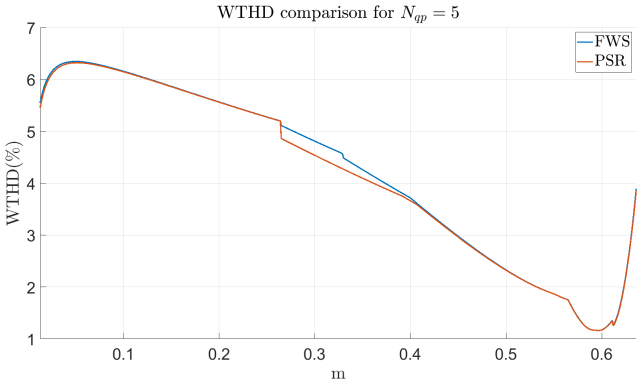

Figure 7: Comparison between FWS and PSR method according to WTHD for $N_{qp} = 5$ when the objective function is WTHD

The curves show that the PSR method provides best solutions than the other ones. For the WTHD objective function, the advantage of PSR method is for m around $\frac{1}{\pi}$ for $N_{qp} = 5$ and around $\frac{1}{\sqrt{3}}$ for $N_{qp} = 2$. Furthermore tables 4 and 5 show an improvement in comparison to other strategies.

Strategy	$N_{qp} = 2$	$N_{qp} = 5$
QWS	8.16%	4.30%
HWS	8.16%	4.26%
FWS	8.11%	4.21%
PSR	8.06%	4.16%

Table 4: Simulation mean value of WTHD for different solutions in percentage according to (35)

N_{qp}	$m = \frac{V_1}{E_{DC}}$	ε
$N_{qp} = 2$	0.53	3.52%
	0.55	7.11%
	0.57	15.85%
$N_{qp} = 5$	0.27	5.02%
	0.3	5.67%
	0.33	4.84%

Table 5: Simulation comparison between FWS and PSR for six specific operating points inside the improvement zone. Percentage of improvement have been computed thanks to (34) and (43).

It is interesting to note that all the symmetries relaxation allow to improve the results. Finally PSR strategy improve FWS with a mean value $V_{WTHD,\%} = 8.06\%$ for $N_{qp} = 2$ and $V_{WTHD,\%} = 4.16\%$ for $N_{qp} = 5$ according to (35). It could seem negligible because all the solutions give the same WTHD, on a wide range of modulation indexes. Nevertheless as it can be seen in Figs. 6 and 7 but also in table 5, the maximum improvement of PSR in terms of WTHD in comparison with FWS is $\varepsilon = 16.15\%$ for $N_{qp} = 2$ and $\varepsilon = 6.37\%$ for $N_{qp} = 5$ according to (43). Then, even if the global mean value affords a small improvement, some operating points improve the WTHD of 16%. Furthermore the improvement zone is not negligible as it covers more than 30% of the feasible operating points.

$$\varepsilon = 100\frac{WTHD_{FWS} - WTHD_{PSR}}{WTHD_{FWS}} \quad (43)$$

6.2. Smoothness

Another criterion identified is the smoothness. To illustrate this criterion Fig. 8 and Fig. 9 show the regularity of the solutions.

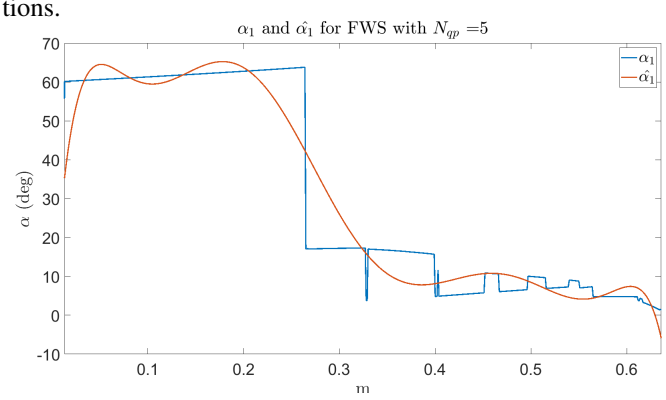

Figure 8: Example of smoothness for the first angle of the WTHD, for the FWS solution with $N_{qp} = 5$

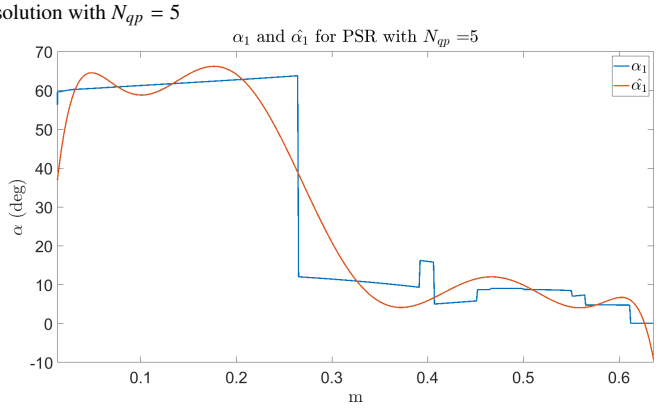

Figure 9: Example of smoothness for the first angle of the WTHD, for the PSR solution with $N_{qp} = 5$

Strategy	$N_{qp} = 2$	$N_{qp} = 5$
QWS	85.6%	84.5%
HWS	85.6%	83.7%
FWS	67.7%	76.1%
PSR	63.8%	86.1%

Table 6: Value of smoothness for different solutions in percentage (computed with WTHD) according to (42)

The smoothness computation has been done with a 8 order polynomial approximation. In this case the smoothness is considered good enough, verified by the smoothness factor given in table 6). In this table QWS affords the best smoothness and PSR the worst one for $N_{qp} = 2$ but for $N_{qp} = 5$ the PSR is the best one.

For QWS and HWS, the smoothness is better than FWS, this is due to the imposed symmetries inside the solutions which reduces the gaps between angles solutions.

Fig. 8 and Fig. 9 illustrate how works the smoothness factor. Indeed those curves are examples for the first angle of the first phase solution set, which is respectively equal to $r_k = 75.2\%$ and $r_k = 89.6\%$ according to (42).

6.3. Switching losses influence

About the influence of PSR on switching losses, it was decided to compute the efficiency of FWS and PSR in simulation for a particular case and compare both of them. The comparison is performed by computing the relative gap between the two efficiencies (49). In the following example the number of phases is also set to $p = 3$.

First, the efficiency η is defined thanks to eq. (44) and eqs.(45)-(48)

$$\eta = \frac{\mathcal{P}_u}{\mathcal{P}_{tot}} \tag{44}$$

P_u designates the useful power and P_{tot} the total one. As the three phases could be different, it is mandatory to compute their power independently.

$$\mathcal{P}_u = \sum_{k=1}^{p} V_{k,1} I_{k,1} \cos(\varphi_{k,1}) \tag{45}$$

$$\mathcal{P}_{tot} = \mathcal{P}_{sw} + \mathcal{P}_{con} + \sum_{k=1}^{p} \sum_{h=1}^{\infty} V_{k,h} I_{k,h} \tag{46}$$

$$\mathcal{P}_{sw} = f_1 \sum_{k=1}^{p} \sum_{j=1}^{N_d} E_{sw} \left(i_k \left(\frac{\mathbf{x}_{k,j}}{\omega} \right) \right) \tag{47}$$

$$\mathcal{P}_{con} = f_1 \sum_{k=1}^{p} \int_0^{\frac{1}{f_1}} S_k(t) P_{con}(i_k(t)) dt \tag{48}$$

Remark that P_{con} and E_{sw} includes the losses of the IGBT and the diode for the two switches composing the leg k.

Thanks to previous equations and arbitrary parameters of R, L, IGBT and diode components [4], it is possible to compare the FWS efficiency η_{FWS} and the PSR efficiency η_{PSR} with eq. (49).

$$\varepsilon_\eta = 100 \frac{\eta_{FWS} - \eta_{PSR}}{\eta_{FWS}} \tag{49}$$

As shown in figures 10a and 10b the influence of angle symmetry relaxation is positive on efficiency for highest operating points when $N_{qp} = 2$. For $N_{qp} = 5$ losses impact is almost negligible, because the impact is lower than 1%. Even if for this last configuration PSR decrease a little the efficiency value in comparison of FWS. These conclusions are not surprising as it is well known that the main influence on the switching losses is the switching frequency f_s. Furthermore a reader who would specifically reduce switching losses or increase efficiency can easily change the objective function in eq.(15) from WTHD to efficiency one or whatever he desires.

In this paper it is shown that the PSR strategy provides best results than FWS one. The superiority of PSR, in simulation, is then established for two purposes, increasing the solution quality and increasing the smoothness quality (as defined in section 5.2) without increasing drastically the switching losses.

[4] $R = 10\text{m}\Omega$; $L = 170\mu\text{H}$;
switch: https://www.onsemi.com/pdf/datasheet/ngtb40n60ihlw-d.pdf

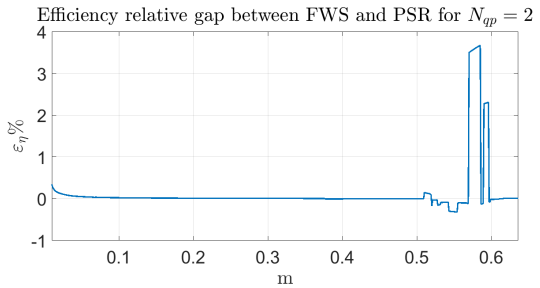

(a) ε_η for $N_{qp} = 2$

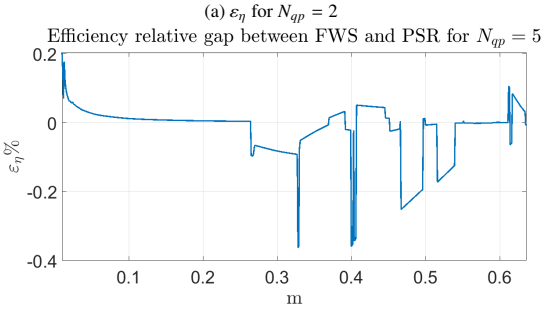

(b) ε_η for $N_{qp} = 5$

Figure 10: Efficiency relative gap for $N_{qp} = 2$ and $N_{qp} = 5$.

7. Experimental results

In order to confirm experimentally the well funded of the proposed strategy, an experimental setting has been set up. It is composed of a DSpace© system (RTI 1103 with MatLab© 2010) that is generating the PWM signals sent to a three legs two levels inverter via I/O ports. Each switch is composed of a MOSFET with two freewheeling diodes. The power of the inverter is provided by a stabilized DC generator of 25V for safety reasons. Then the inverter is connected to a balanced three-phases inductive load composed with $R \approx 12.9\Omega$, $L \approx 1.2$H.

Remark that the angular precision in simulation section is equal to $100\pi \cdot 10^{-6}$ rad for an electrical frequency of 50Hz. Then in order to at least respect this angular precision and the experimental device limitations, the experimental electrical frequency is set to 1Hz. Indeed a technical limitation of the microcontroller sampling period equal to 30µs. By doing so the angular precision is equal to $60\pi \cdot 10^{-6}$ rad, which is lower than the simulation one. Since the simulink scheme is real time the dead-time is equal to one step of controller computation and then is equal to 30µs≡ 60πµrad

Concerning the voltage measurement, a Rohde Swartz's© probe is used and connected between the input of the RL load and the neutral point. The voltage is sent to the DSpace, by saving datas for ten periods (i.e. 10s). Then the harmonic spectrum of the voltage is extracted and finally the WTHD is computed by using equation (34). A video of the experimental bench can be found in [35] and on figure 11, the parameters are sum up in table 7.

In the table 9, three specific points where selected for $N_{qp} = 2$ and $N_{qp} = 5$, with respect to the improvement zone visible on Figs. 6 and 7. The table results are computed with (43), and show a WTHD improvement of the PSR against the FWS.

In order to verify the behavior of the PSR against the FWS

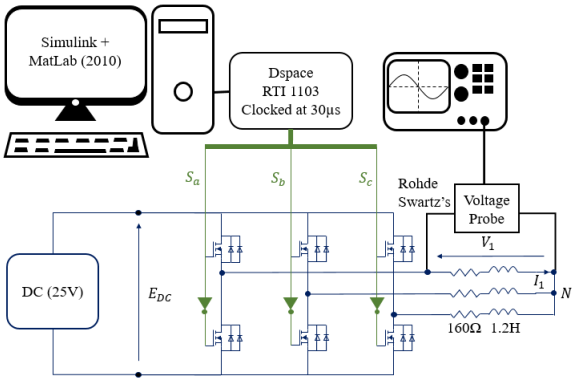

Figure 11: Schematic representation of the experimental bench.

Parameter	Value
f_1	1Hz
δt_{min}	30µs
Δt	60µs
E_{DC}	25V
R	12.9Ω
L	1.2H

Table 7: Experimental parameters

in all the validity domain. Other operating points are evaluated and are represented on Figs. 12 and 13. The shape of the curves is very similar to the simulation ones (Figs. 6 and 7). Thanks to these experiments a mean value of improvement was also computed and the results have been compiled in the table 8. As for simulation results the mean increase is not that much impressive, but, by considering a local improvement with table 9, the value of the PSR strategy is then much more visible.

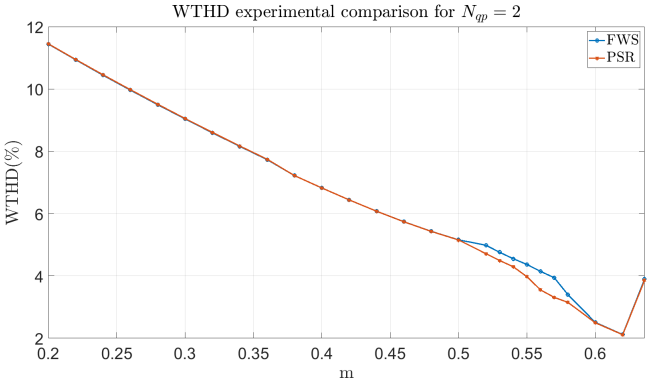

Figure 12: WTHD value for $N_{qp} = 2$, the points have been computed with a step of 0.02

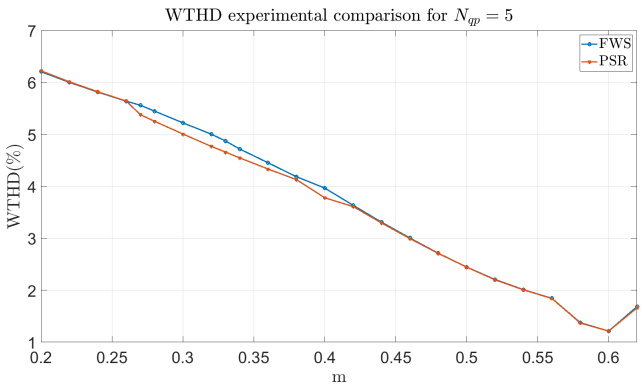

Figure 13: WTHD value for $N_{qp} = 5$, the points have been computed with a step of 0.02

Strategy	$N_{qp} = 2$	$N_{qp} = 5$
FWS	6.44%	3.85%
PSR	6.34%	3.79%

Table 8: Experimental mean value of WTHD for FWS and PSR in percentage. This percentage was computed with the same points than Figs. 12 and 13.

N_{qp}	$m = \frac{V_1}{E_{DC}}$	ε
$N_{qp} = 2$	0.53	5.53%
	0.55	9.03%
	0.57	16.02%
$N_{qp} = 5$	0.27	3.28%
	0.3	4.12%
	0.33	4.39%

Table 9: Experimental comparison between FWS and PSR

for six specific operating points inside the improvement zone. Percentage of improvement have been computed thanks to (34) and (43).

Experimental results confirm the superiority of the PSR method against QWS, HWS or a FWS for low N_{qp}. For higher N_{qp} the results are similar for all the considered methods because significant voltage harmonics of eq. (34) would be in high enough frequency to be negligible.

Experimental results are also validated thanks the simulation ones as table 4 corroborates with table 8, but also table 5 is similar in terms of improvement to 9.

As the experimental results depends on dead-time, it is shown there is no significant influence of Δt on experimental results. Nevertheless for higher electrical frequencies, it would be necessary to start again an optimization in order to ensure this kind of solutions quality (see fig. 16). Indeed an increase of electrical frequency will also decrease the angular precision as δt_{min} is set to 1µs.

Fig. 14 is the Fourier transform of the phase voltage of Fig. 15 obtained with $N_{qp} = 2$ and $m = 0.57$. It can be seen from Fig. 14 in red color (PSR) the harmonics multiple of three are not removed (see zoom on first harmonics), which confirms the relaxations constraint of angle symmetry between phases (see eq. (11) and the comment below) for PSR strategy.

About general implementation issues of classical methods and PSR method, the computed angles have to be stored inside

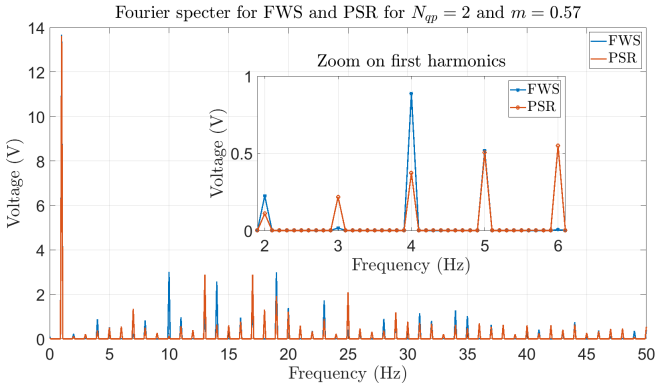

Figure 14: Fourier spectrum for the FWS and PSR for $N_{qp} = 2$ and $m = 0.57$.

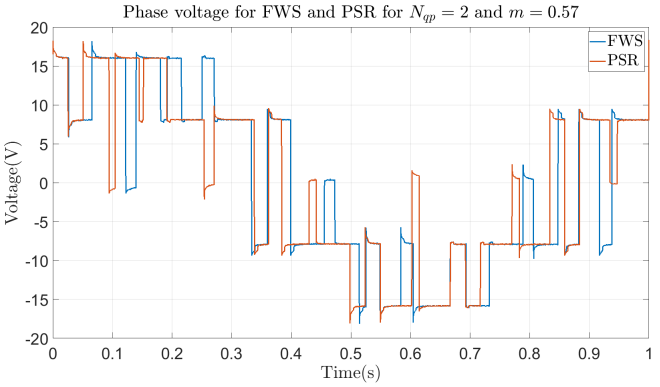

Figure 15: Voltage waveform for the FWS and PSR for $N_{qp} = 2$ and $m = 0.57$.

a micro controller [11, 36]. The controller always reads the tables and send an interruption when the internal clock value (converted in angles) corresponds to the table one (Fig. 16). As the precision is function of the sampling time and electrical frequency, it is necessary for the same precision to increase the speed of a micro controller if the electrical frequency increases. In the same way of thinking for a fixed controller speed the precision can be increased by lowering the electrical frequency, which is done in this section. It is important to remark that the storage of PSR is three times greater than the one of FWS and twelve times greater than the one of QWS. Nevertheless, the size of the tables is still technologically and economically acceptable.

Even if the previous example is dedicated to three phases RL load, the proposed strategy can be used for p-phases and any inductive or capacitive load.

8. Conclusion

In this paper a proposition of a new PWM method with a relaxation of symmetry for low switching frequency, called Phases Symmetry Relaxation (PSR) was done. A simulation evaluation of this strategy was performed according to WTHD compared with classical PWM symmetry strategies for the specific case of a three phases voltage inverter. Furthermore experimental results corroborates the first results obtained in simulation for the same conditions.

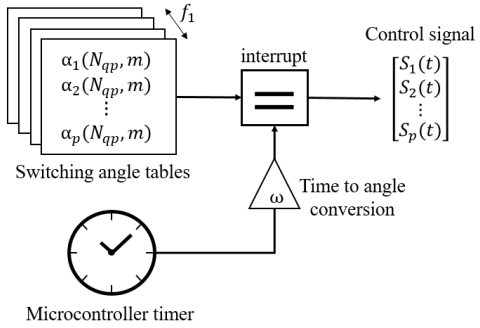

Figure 16: Off-line PWM control in the particular case of a three phase inverter. Solutions depends also on fundamental frequency for the angular precision. For this third dimension, each table should be understood as a frequency interval and not as a specific frequency.

For all the studied operating points, PSR strategy affords the best results in comparison with the classical OPPs solutions as FWS, described in [11]. Indeed computation and experiments performed shows an improvement of WTHD for some specific modulation index and for low switching frequency.

As a generic optimization problem was defined without specific load, it was highlighted that PSR method can be applied to a p-phases inverter to feed either an inductive (voltage WTHD) or a capacitive load (current WTHD). Furthermore a new smoothness criterion (Evaluates the smoothness of the switching angles when the modulation index changes) was presented and simulation results shown that PSR is competitive with other OPPs.

In future works experimental validation of the proposed strategy will be done on a synchronous electric motor, which implies a variation of the electrical frequency and modulation index dynamically. Furthermore even if WTHD and smoothness are the most important criteria, some other criteria could be interesting to study in future works. In addition, the WTHD optimization related to PSR probably underestimate the benefits of the technique. Indeed on a motor with a non sinusoidal electromotive force, the interest is intuitively better for PSR as it plays with the phases symmetry. Nevertheless showing the PSR improve the WTHD is an important step as it is easy to understand and classic for OPP considerations especially thanks with the generic optimization proposed.

References

[1] D. Holmes, T. Lipo, Pulse Width Modulation for Power Converters: Principles and Practice, Wiley-IEEE Press, 2003.

[2] A. Kernick, J. L. Roof, T. M. Heinrich, Static inverter with neutralization of harmonics, Transactions of the American Institute of Electrical Engineers, Part II: Applications and Industry 81 (2) (1962) 59–68. doi:10.1109/TAI.1962.6371793.

[3] J. Holtz, Pulsewidth modulation for electronic power conversion, Proceedings of the IEEE 82 (8) (1994) 1194–1214.

[4] J. Holtz, Advanced pwm and predictive control - an overview, IEEE Transactions On Industrial Electronics 63 (6) (2016) 3837–3844.

[5] M. Bouarfa, A. Bodson, M. Fadel, An optimization formulation of converter control and its general solution for the four-leg two-level inverter, IEEE Transactions on Control Systems Technology 26 (5) (2018) 1901–1908. doi:10.1109/TCST.2017.2738608.

[6] S. Capitaneanu, B. de Fornel, M. Fadel, J. Faucher, A. Almeida, Graphical and algebraic synthesis for pwm methods, EPE Journal 11 (3) (2001) 16–28. doi:10.1080/09398368.2001.11463485.

[7] A. M. Bozorgi, M. Monfared, H. R. Mashhadi, Optimum switching pattern of matrix converter space vector modulation, in: 2012 2nd International eConference on Computer and Knowledge Engineering (ICCKE), 2012, pp. 89–93. doi:10.1109/ICCKE.2012.6395358.

[8] K. Zhou, D. Wang, Relationship between space-vector modulation and three-phase carrier-based pwm: a comprehensive analysis [three-phase inverters], IEEE Transactions on Industrial Electronics 49 (1) (2002) 186–196. doi:10.1109/41.982262.

[9] Z. Gao, T. Chen, C. Zhang, Control of an active bus voltage limiter with modified space vector pulse width modulation strategies in regenerative applications, Control Engineering Practice 83 (2019) 176–187.

[10] M. S. A. Dahidah, G. Konstantinou, V. G. Agelidis, A review of multilevel selective harmonic elimination pwm: Formulations, solving algorithms, implementation and applications, IEEE Transactions on Power Electronics 30 (8) (2015) 4091–4106. doi:10.1109/TPEL.2014.2355226.

[11] A. Birth, T. Geyer, H. du Toit Mouton, M. Dorfling, Generalized three-level optimal pulse patterns with lower harmonic distortion, IEEE Transactions on Power Electronics 35 (6) (2019) 5741–5752.

[12] N. Hartgenbusch, R. W. De Doncker, A. Thünen, Optimized pulse patterns for salient synchronous machines, in: 2020 23rd International Conference on Electrical Machines and Systems (ICEMS), 2020, pp. 359–364. doi:10.23919/ICEMS50442.2020.9290786.

[13] S. K. Pandey, S. L. Patil, D. Ginoya, U. M. Chaskar, S. B. Phadke, Robust control of mismatched buck dc–dc converters by pwm-based sliding mode control schemes, Control Engineering Practice 84 (2019) 183–193.

[14] R. Madonski, K. Łakomy, M. Stankovic, S. Shao, J. Yang, S. Li, Robust converter-fed motor control based on active rejection of multiple disturbances, Control Engineering Practice 107 (2021) 104696.

[15] M. Arahal, F. Barrero, S. Toral, M. Duran, R. Gregor, Multi-phase current control using finite-state model-predictive control, Control Engineering Practice 17 (5) (2009) 579–587.

[16] J. Vilain, C. Lesbroussart, Une nouvelle stratégie de modulation du vecteur d'espace pour un onduleur de tension triphasé: La modulation delta sigma vectorielle, Journal de Physique III 5 (7) (1995) 1075–1088.

[17] R. Vazquez, F. Gavilan, E. F. Camacho, Pulse-width predictive control for ltv systems with application to spacecraft rendezvous, Control Engineering Practice 60 (2017) 199–210.

[18] A. Edpuganti, A. K. Rathore, A survey of low switching frequency modulation techniques for medium-voltage multilevel converters, IEEE Transactions on Industry Applications 51 (5) (2015) 4212–4228. doi:10.1109/TIA.2015.2437351.

[19] J. Lago, M. L. Heldwein, Generalized synchronous optimal pulse width modulation for multilevel inverters, IEEE Transactions on Power Electronics 32 (8) (2017) 6297–6307. doi:10.1109/TPEL.2016.2621022.

[20] E. Sournac, Variateur de vitesse pour machine asynchrone commande numérique et stratégies mli, optimisation des modulations, Ph.D. thesis, ENSEEIHT, Laboratoire d'Electrotechnique et d'Electronique Industrielle (1990).

[21] K. Shi, H. Li, Optimized random pwm strategy based on genetic algorithms, in: IECON'03. 29th Annual Conference of the IEEE Industrial Electronics Society (IEEE Cat. No.03CH37468), Vol. 1, 2003, pp. 7–11 vol.1. doi:10.1109/IECON.2003.1279946.

[22] K. Shi, H. Li, Optimized pwm strategy based on genetic algorithms, IEEE Transactions on industrial electronics 52 (05) (2005) 1458–1461.

[23] X. Fei, W. Ruan, B. Wu, A generalized formulation of quarter-wave symmetry she-pwm problems for multilevel inverters, IEEE Transactions on Power Electronics 24 (7) (2009) 1758–1766.

[24] J. Birda, A.D. Reuss, C. Hackl, Synchronous optimal pulse-width modulation with differently modulated waveform symmetry properties for feeding synchronous motor with high magnetic anisotropy, ReseachGate, Working Copy (2017).

[25] H. Hosseinnia, D. Nazarpour, Utilization of a novel meta heuristic algorithm to minimize total harmonic distortion, Majlesi Journal of Electrical Engineering 12 (3) (2018) 77–84.

[26] Y. Sahali, M. Fellah, Selective harmonic elimination pulse-width modulation technique (she pwm) applied to three-level inverter / converter, IEEE (2003) 1112–1117.

[27] F. G. Turnbull, Selected harmonic reduction in static d-c — a-c invert-

ers, IEEE Transactions on Communication and Electronics 83 (73) (1964) 374–378. doi:10.1109/TCOME.1964.6541241.

[28] H. S. Patel, R. G. Hoft, Generalized techniques of harmonic elimination and voltage control in thyristor inverters: Part i–harmonic elimination, IEEE Transactions on Industry Applications IA-9 (3) (1973) 310–317. doi:10.1109/TIA.1973.349908.

[29] H. S. Patel, R. G. Hoft, Generalized techniques of harmonic elimination and voltage control in thyristor inverters: Part ii — voltage control techniques, IEEE Transactions on Industry Applications IA-10 (5) (1974) 666–673. doi:10.1109/TIA.1974.349239.

[30] J. Sun, S. Beineke, H. Grotstollen, Optimal pwm based on real-time solution of harmonic elimination equations, IEEE Transactions on Power Electronics 11 (4) (1996) 612–621. doi:10.1109/63.506127.

[31] M. S. A. Dahidah, V. G. Agelidis, Selective harmonic elimination pwm control for cascaded multilevel voltage source converters: A generalized formula, IEEE Transactions on Power Electronics 23 (4) (2008) 1620–1630. doi:10.1109/TPEL.2008.925179.

[32] A. Bourgeade, M. Ghanes, M. Fadel, A. Bouarfa, J.-P. Barbot, Off-line pwm control with a three phases relaxed symmetry applied to a two-level inverter, in: 2021 IEEE Conference on Control Technology and Applications (CCTA), 2021, pp. 595–600. doi:10.1109/CCTA48906.2021.9659137.

[33] T. Itkonen, J. Luukko, A. Sankala, T. Laakkonen, R. PÖllÄnen, Modeling and analysis of the dead-time effects in parallel pwm two-level three-phase voltage-source inverters, IEEE Transactions on Power Electronics 24 (11) (2009) 2446–2455. doi:10.1109/TPEL.2009.2033064.

[34] M. Sierra, C. Coello, Improving pso-based multi-objective optimization using crowding, mutation and ϵ-dominance, Evolutionary Multi-Criterion Optimization, Third international Conference EMO (2005) 505–519.

[35] A. Bourgeade, M. Ghanes, M. Fadel, A. Bouarfa, J.-P. Barbot, R. Boisliveau, Phases symmetry relaxation (PSR) experimental plateform (https://youtu.be/995fgSWSobk) (2021).
URL `https://youtu.be/995fgSWSobk`

[36] D. O. Neacşu, Y. Zheng, B. Lehman, An sd card flash-memory-based implementation of a multioptimal three-phase pwm generator, IEEE Transactions on Power Electronics 31 (1) (2016) 39–51. doi:10.1109/TPEL.2015.2424200.